Synthesis of Xenon and Iron-Nickel Intermetallic Compounds at Earth's Core Thermodynamic Conditions

Elissaios Stavrou, Yansun Yao, Alexander F. Goncharov, Sergey S. Lobanov, Joseph M. Zaug, Hanyu Liu, Eran Greenberg, and Vitali B. Prakapenka

Synthesis of Xenon and Iron/Nickel intermetallic compounds at Earth's core thermodynamic conditions

Elissaios Stavrou,[1, *] Yansun Yao,[2, 3, †] Alexander F. Goncharov,[4, 5, 6, ‡] Sergey Lobanov,[5, 7]

Joseph M. Zaug,[1] Hanyu Liu,[5] Eran Greenberg,[8] and Vitali B. Prakapenka[8]

[1]*Lawrence Livermore National Laboratory,*

Physical and Life Sciences Directorate, Livermore, California 94550, USA

[2]*Department of Physics and Engineering Physics,*

University of Saskatchewan, Saskatoon Saskatchewan, S7N 5E2, Canada

[3]*Canadian Light Source, Saskatoon, Saskatchewan, S7N 2V3, Canada*

[4]*Key Laboratory of Materials Physics and Center*

for Energy Matter in Extreme Environments,

Chinese Academy of Sciences, Hefei 230031, China

[5]*Geophysical Laboratory, Carnegie Institution*

of Washington, Washington, D.C. 20015, USA

[6]*University of Science and Technology of China, Hefei, 230026, China*

[7]*V.S. Sobolev Institute of Geology and Mineralogy,*

SB RAS,3 Pr. Ac. Koptyga, Novosibirsk 630090, Russia.

[8]*Center for Advanced Radiation Sources,*

University of Chicago, Chicago, IL 60637, USA

(Dated: January 3, 2018)

Abstract

Using in situ synchrotron X-ray diffraction and Raman spectroscopy in concert with first principles calculations we demonstrate the synthesis of stable $Xe(Fe,Fe/Ni)_3$ and $XeNi_3$ compounds at thermodynamic conditions representative of Earth's core. Surprisingly, in the case of both the Xe-Fe and Xe-Ni systems Fe and Ni become highly electronegative and can act as oxidants. The results indicate the changing chemical properties of elements under extreme conditions by documenting that electropositive at ambient pressure elements could gain electrons and form anions.

Noble gas elements (NGEs) are considered as the most chemically inert elements due to the closed subshells configuration that prevents the formation of stable compounds. However, recent theoretical studies [1–4] suggest that stable compounds between NGEs and metals (electropositive at ambient conditions elements) could be formed under high pressure conditions due to the substantial effect of pressure on the chemical properties. The stability of such compounds can be attributed to the changes of chemical properties of elements under pressure [1, 5–7]. This includes altered electronegativity and reactivity, charge transfer between orbitals and/or constitution elements, and the appearance of multicenter bonding and electride states [8]. In general, for the predicted stable compounds of NGEs and metals a NGE can either gain electrons from an electropositive, at the corresponding pressures, element [3]or a metal becomes electronegative and acts as an oxidant (e.g. Xe-Fe/Ni system [1]). The latter case is unusual and counters chemical intuition because it implies that Fe and Ni become more electronegative than Xe. Experimental realization of such compounds is incomplete highlighting the necessity of experimental verification of theory to better understanding of the chemistry at extreme conditions and thus, advancing chemistry and physics of highly compressed material states.

The formation of stable Xe-Fe(Ni) compounds would also change our understanding about the presence of Xe in the Earth's core. According to the simple mass fractionation model (see discussion in Ref. [9, 10] and references therein), heavy NGEs should be less depleted and isotopically fractionated in comparison to the lighter ones, in agreement to observations in meteorites. However, in the Earth's atmosphere, Xe is more depleted than Kr and more fractionated than both Kr and Ar [9]. These two observations constitute one of the most challenging open questions in the geosciences [9, 11], and give rise to the so-called "missing Xe paradox". Although various models have been suggested on the origin of the Xe depletion[12], it is commonly attributed to the inclusion of Xe in the Earth's interior [10]. While Xe was reported to form compounds with water ice [13] and quartz [14], none of them provide a plausible explanation to the "missing Xe paradox"[15]. The successful formation of xenon oxides under deep mantle conditions has been recently reported [16]. However, the presence of such compounds is precluded by the lack of free oxygen in Earth's mantle.

Accordingly, a hypothesis of stable Xe-Fe/Ni compounds in the Earth's core was proposed as an explanation for the "missing" Xe [10]. In this scenario, other NGEs are not "missing" due to the much more extreme thermodynamic conditions needed for the formation

of stable compounds [3]. Previous experimental attempts didn't trace formation of Fe-Xe compounds up to 200 GPa and below 2500 K [17–19] and this has been attributed to the large size difference between Xe and Fe ions, which hinders the formation of Xe-Fe solid solutions according to the Hume-Rothery rule [18]. A recent theoretical study [1], using *ab-initio* calculations combined with structural search methods, suggests that Xe-Ni and Xe-Fe compounds are thermodynamically stable above 150 GPa and 200 GPa respectively. The stability of these compounds is enhanced at elevated temperatures (>2000 K) *i.e.* at thermodynamic conditions representative of Earth's outer core. The predicted crystal structures of Xe-Fe/Ni compounds are distinct from the structures of elemental Xe, Fe, and Ni at the same thermodynamic conditions. This suggests that the formation mechanism of these compounds goes beyond a simple element substitution.

In this study, we explored the possible formation of stable compounds in the Xe-Fe/Ni system at thermodynamic conditions representative of the Earth's core by performing high pressure experiments in a laser-heated (LH) diamond-anvil cell (DAC) starting from the following mixtures: a)Xe-Fe, b) Xe-Fe/Ni alloy ($\sim$ 7% Ni) and c) Xe-Ni. Using *in situ* synchrotron X-ray diffraction (XRD) and Raman spectroscopy we successfully identified the formation of: a) a $XeFe_3/Xe(Fe_{0.93}Ni_{0.07})_3$ compound, characterized as a mixture of a FCC and an orthorhombic $NbPd_3$-type structures, above 200 GPa and 2000 K and b) a $XeNi_3$ compound, in the form of a $CrNi_3$-type FCC structure, above 150 GPa and 1500 K. Preliminary data on all these observations have been reported at the AGU 2015 Fall meeting [20]. We find the formation of $XeFe_3$ compounds above 200 GPa (in contrast with previous studies [19]) while $XeNi_3$ forms at much lower pressure signifying the importance of the elemental electronic structure. The experimental results were examined and supported in synergy with theoretical *ab-initio* structural search and optimization. The formation of $XeFe_3$ and $XeNi_3$ compounds are kinetically driven with the structures identified in close proximity to the computed energy minima. The theoretical reaction threshold pressures for both compounds are in very good agreement with the experiment.

For the case of the Fe-Ni alloy with a Ni concentration (7-8%) representative of the Earth's core [21, 22] an iron Sikhote-Alin Meteorite was used as a proxy after chemical and homogeneity characterization using EDX spectroscopy (see Fig.1 of the Supplemental Material [23]). The XRD patterns of the Fe-Ni alloy used in this study are representative of a HCP structure (see Fig 1(a)) with negligible cell volume difference (Fig. S2), at a given

3

pressure, to that of pure Fe (also in HCP structure) in agreement with previous studies [24]. We performed LH experiments on both the Xe-Fe and Xe-Fe$_{0.93}$Ni$_{0.07}$ systems at various pressures from 150 to above 210 GPa. No new Bragg peaks, signalling the formation of new compounds, were observed below 195 GPa even after a prolonged LH above 3500 K, see Fig. S3. However, new Bragg peaks appeared for both mixtures after LH at $\sim$2200 K and pressures >200 GPa, implying an approximately 200 GPa reaction threshold, see Fig. 1(a) and Fig. S4(b). XRD patterns of the Xe-Fe and Xe-Fe$_{0.93}$Ni$_{0.07}$ systems after LH (Fig. S4(a)) are essentially identical. Thus, we suggest that the presence of a low-concentration of Ni in the Fe-Ni alloy has no effect on the structure of the synthesized compound. Bragg peaks of pure Ni or a Fe$_{0.97}$Ni$_{0.07}$ BCC structure [21] were not observed during or after LH. Consequently, the possibility of phase separation or a phase transition are ruled out.

The new peaks in XRD patterns after LH of the Xe-Fe and Xe-Fe$_{0.97}$Ni$_{0.07}$ mixtures cannot be indexed solely with the FCC (*Pm-3m*) XeFe$_3$ structure (Cu$_3$Au type) predicted by Zhu et al. [1] due to a much higher number of observed Bragg peaks and the presence of low angle peaks (see Fig. 1(a)). Moreover, no Raman active modes are expected for the Cu$_3$Au-type structure in contrast with our Raman spectroscopy measurements (Fig. S5(a)). We identified the products as a mixture of a FCC and an orthorhombic (namely *Pmmn* (1)) phases with competitive enthalpies as revealed in our theoretical calculations, Fig. 2(a). Details on the procedure we followed for the identification of the *Pmmn* (1) phase can be found in the Supplemental Material together with the relevant structural parameters including Wyckoff positions, see Table S1. The *Pmmn* (1) and the FCC structures are closely related as both are close-packed with 12-fold coordinated Fe and Xe atoms. As a result, the volumes of these two structures are essentially degenerate above 100 GPa (Fig. 1(c)).

The Bragg peaks of the experimental XRD patterns can be very well indexed with a mixture of *Pmmn (1)* and *Pm-3m* structures. However, preferred orientation and strongly anisotropic peak broadening effects, usual in HP-HT synthesis [25], prevent us from a full structural refinement (Rietveld) of the positional parameters due to differences between the observed and calculated intensities. Difference in relative intensities could also arise from a positional disordered phase. For this reason, we have considered a positionally disordered *Pmmn (1)* structure with a Xe(25%)-Fe (75%) site occupancy. This structure has a negligible enthalpy difference with the ordered *Pmmn (1)* one and provides a better agreement with
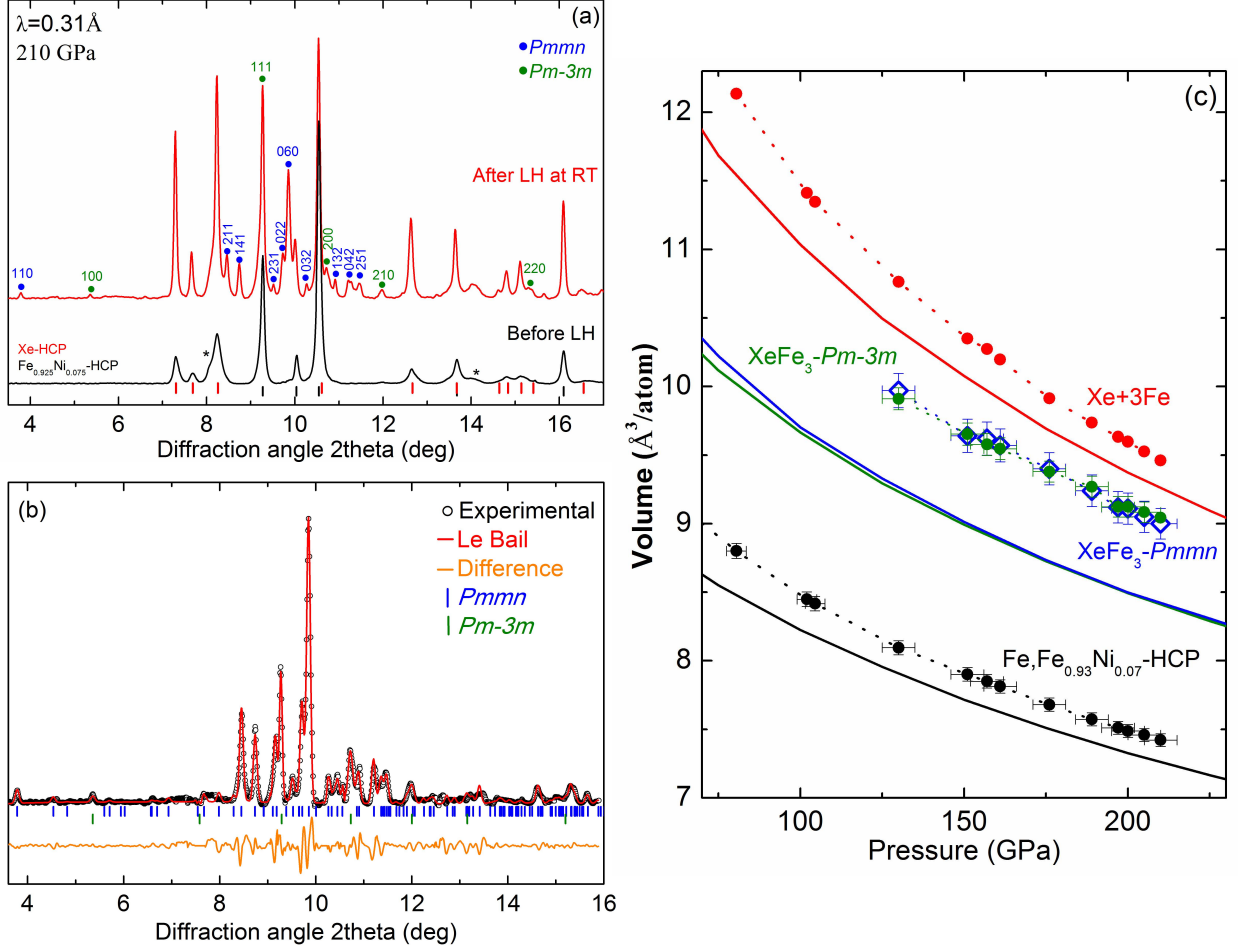
FIG. 1. a) XRD patterns of the Xe-$Fe_{0.93}Ni_{0.07}$ mixture before and after LH at 210 GPa. New Bragg peaks after LH and corresponding Miller indices for the *Pm-3m* and the *Pmmn* $XeFe_3$ crystal structures are noted with green and blue circles respectively. The peak marked by the asterisk corresponds to the strongest peak of rhenium (gasket material). (b) Le Bail refinement of the $Xe(Fe_{0.93}Ni_{0.07})_3$ compound at 210 GPa. The peaks of *Pm-3m* and *Pmmn* (1) structures are marked with green and blue vertical lines, respectively. (c) EOSs of Fe and $XeFe_3$/$Xe(Fe_{0.93}Ni_{0.07})_3$ as determined experimentally (dashed curves and solid symbols) and theoretically (solid curves) in this study. The volume of the superposition of (Xe+3Fe)/4 is also shown for comparison.The X-ray wavelength is $\lambda=0.31$Å.

the experimental XRD patterns at the low 2θ (high-d) range *i.e.* the range that is mainly affected by a difference between an ordered and a positionally disordered structure. In Fig. 1(b) we show the Le Bail refinement of the experimentally observed diffraction pattern based on a mixture of *Pmmn* (1) (with Xe(25%)-Fe (75%)) and *Pm-3m* structures, after
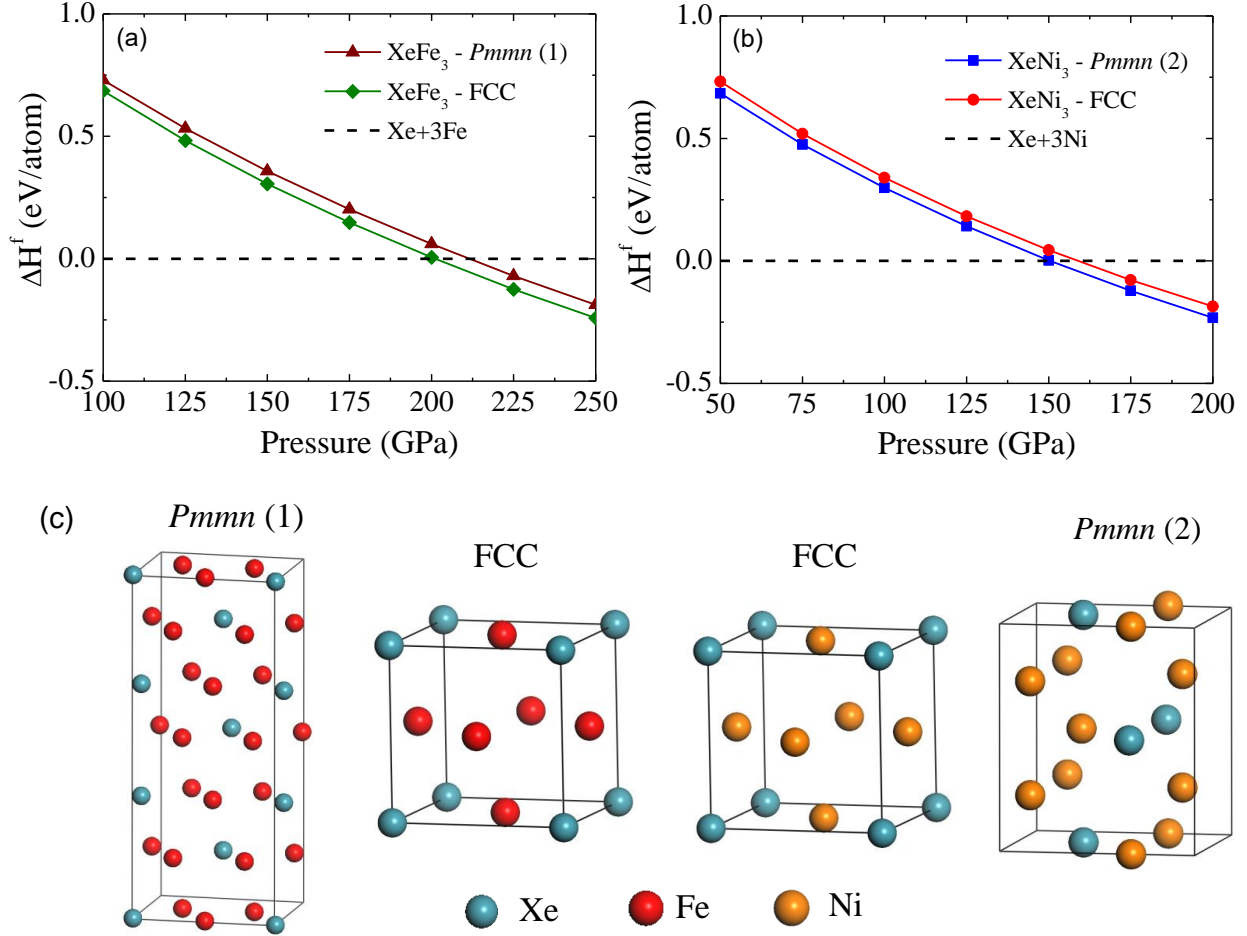
5

FIG. 2. Calculated enthalpies of formation ΔH^f of: (a) XeFe$_3$ and (b) XeNi$_3$ with respect to the mixture of elemental Xe + 3Ni and Xe + 3Fe, respectively. The enthalpies of the FCC structure in both compounds were calculated in an ordered structure. The two *Pmmn* structures in XeFe$_3$ and XeNi$_3$ are distinctly different and therefore distinguished as *Pmmn* (1) and *Pmmn* (2). (c) Schematic representations of the corresponding structures of XeFe$_3$ and XeNi$_3$.

subtracting (see Ref. [26] and Fig. S3(c) for a representative example) the Fe and Xe related Bragg peaks.

Raman experiments on samples quenched to 300 K (Fig. S5(a)) show the presence of a new broad weak peak at 450-480 cm^{-1}. Low intensity Raman spectra are consistent with the formation of a metallic or semi-metallic XeFe$_3$ compound [1] and consequently only the highest intensity peaks are expected to be observed. The position of the observed Raman peak is indeed in agreement with the strongest calculated peak of the *Pmmn (1)* XeFe$_3$ phase. The FCC XeFe$_3$ compound is not expected to have any Raman activity. Thus the

presence of the Raman bands strongly supports the existence of a second $Pmmn$ (1) phase in addition to FCC XeFe$_3$. Moreover, the pressure slope of the experimentally observed peak and of the most intense peak of the calculated Raman spectrum (Fig. S5(b)) agree well, thus, providing an additional argument in favor of the synthesis of the $Pmmn$ (1) XeFe$_3$ phase.

The experimentally determined volume of XeFe$_3$, is 5% lower than that of the 1:3 solid mixture of Xe and Fe and the theoretical EOS yields the same trend, with the XeFe$_3$ having 8% smaller volume than the mixture, see Fig. 1(c). Compared to the experimental values, the theoretical volumes of Fe and XeFe$_3$/Xe(Fe$_{0.93}$Ni$_{0.07}$)$_3$ are clearly underestimated. Here a possible source of error is the well-known insufficiency of standard DFT treating the ground state of Fe, which was shown to be largely affected by dynamical many-body effects [27]. Nevertheless, experiment and theory agree in that XeFe$_3$ has a smaller volume than its constituents, suggesting, together with the lower enthalpy, that this compound is thermodynamically favored. On pressure release, both the XeFe$_3$ and the Xe(Fe$_{0.93}$Ni$_{0.07}$)$_3$ compounds remain stable down to, at least, 127 GPa (Fig. S6) followed by a decomposition to Xe and Fe/Fe$_{0.93}$Ni$_{0.07}$ at lower pressures.

Figure 3(a) shows XRD patterns of the Xe-Ni mixture at 155 GPa before LH, upon increasing temperature and at RT after LH. The XRD pattern before LH is representative of a heterogeneous mixture of HCP-Xe [28] and FCC-Ni. With increasing temperature the Ni Bragg peaks completely disappear above 1500 K while new peaks appear concomitantly suggesting that Ni fully reacts towards the formation of a new compound that remains stable after quenching to RT. Xe related Bragg peaks remain present suggesting conditions of Xe excess in the cavity. The new Bragg peaks can be indexed with an A1 FCC unit-cell and with a cell volume representative of a XeNi$_3$ compound. This attribution is based on the comparison between the atomic volumes of the synthesized compound, Ni and Xe at the same pressure (see Fig. S7 and Fig. S8(b)). Fulfillment of the extinction conditions of A1 by the observed reflections implies the formation of a CrNi$_3$-type binary alloy with Xe and Ni distributed randomly/statistically over the FCC sites. An ordered FCC structure (Cu$_3$Au-type) would have several additional low intensity Bragg peaks (see Fig. 3(b)), which are absent in the XRD pattern of XeNi$_3$.

The synthesized XeNi$_3$ compound remains stable up to at least 100 GPa upon pressure release, see Fig. S8(a). Significantly, both the experimentally determined and calculated
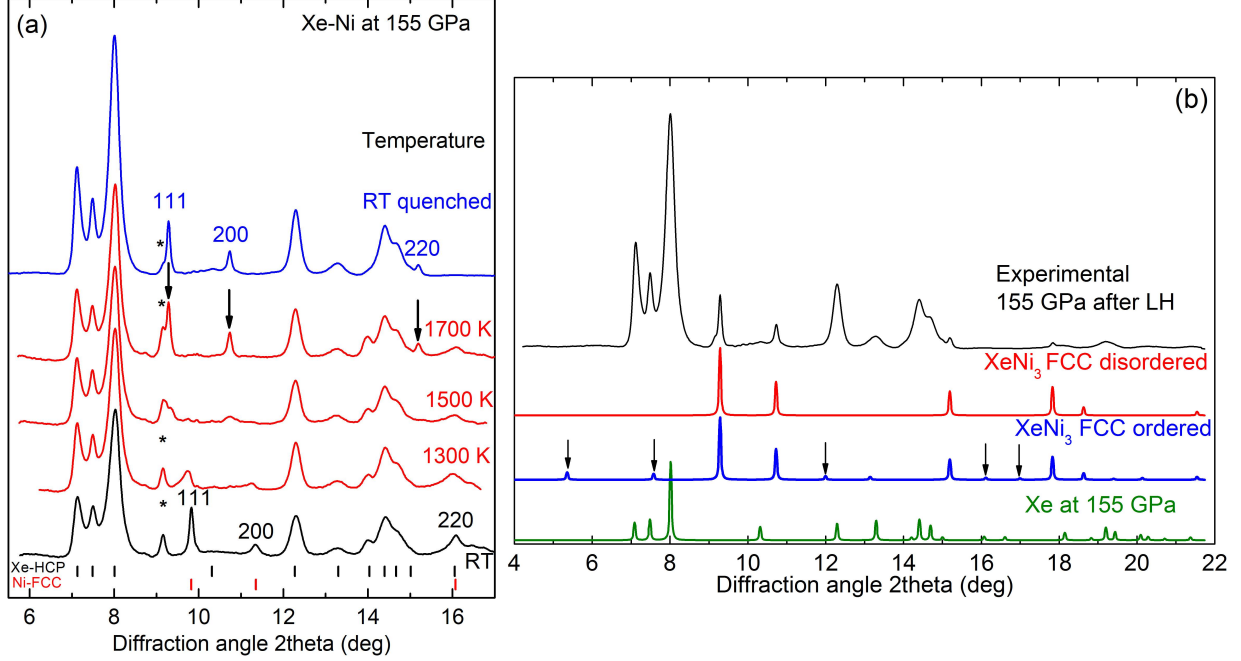
7

FIG. 3. a) XRD patterns of Xe-Ni mixture at 155 GPa as a function of temperature. The peak marked by the asterisk corresponds to the strongest peak of rhenium. The peaks of the hcp-Xe and FCC-Ni at RT before LH are marked with black and red vertical lines, respectively. The vertical arrows mark the position of the Bragg peaks of the $XeNi_3$ compound. The corresponding Miller indices for the FCC-Ni and the FCC-$XeNi_3$ are noted before and after LH respectively. b) XRD pattern of the synthesized $XeNi_3$ compound in comparison to the calculated patterns of ordered (blue) and disordered (red) FCC crystal structures. The calculated pattern of the hcp-Xe is also shown for comparison. The vertical arrows mark the position of the additional Bragg peaks expected in an ordered Cu_3Fe-type FCC. The X-ray wavelength is 0.310 Å.

volume of $XeNi_3$ is ~10% smaller than that of the 1:3 solid mixture of Xe and Ni, suggesting that the former is a stable compound (Fig. S7(b)). However, exact stoichiometry of the synthesized compound may not be precisely determined. Nevertheless, both the experimentally determined EOS and the predicted stability of the $XeNi_3$ compound strongly suggest a composition very close, if not exact, to $XeNi_3$. The thermodynamic stability of the $XeNi_3$ compound was investigated through the relative enthalpy of formation, ΔH^f, with respect to a 1:3 solid mixture of Xe and Ni (Fig. 2(b)). The FCC structure is comparable in enthalpy with the *Pmmn* structure (named here as *Pmmn* (2)) predicted by Zhu et. al. [1]. The

ΔH^f of the FCC structure is slightly higher than the latter one, *i.e.*, by ∼0.04 eV/atom, indicating a metastable structure close to the global minimum.

Considering that the formation of $XeNi_3$ only takes place at high temperature it is reasonable to suggest that the synthesis of this compound is kinetically-driven [29, 30]. The ΔH^f of the FCC structure approaches zero near 158 GPa, which corresponds very well with the experimental reaction threshold of 155 GPa. Both FCC and *Pmmn* (2) structures are close-packed with 12-fold coordinated Ni and Xe atoms (Fig. 2(c)), which explains their similar enthalpies. The enthalpy change due to the positional disorders of Xe and Ni was estimated using a FCC supercell of 256 atoms. A set of 200 structures were generated by placing Xe and Ni atoms randomly at the FCC lattice sites; each representing a possible solid solution configuration. The calculated enthalpies of these structures (at 150 GPa) is within a 0.1 eV/atom range above the enthalpy of the ordered FCC structure.

Recently, Dewaele *et al.* [19] reported the synthesis of a stable $XeNi_3$ compound with an ordered FCC structure. Although the reported stoichiometry, the reaction threshold, the volume per atom and the fundamental crystal structure are in agrement with this work (see also Ref. [20]) a discrepancy exists on the detailed crystal structure *i.e.* ordered vs disordered FCC. This can be attributed to differences in the quenching time. The formation of an ordered structure requires substantial atomic diffusion, which is likely restricted by the fast kinetics in the present case, *i.e.*, the quenching process. Strictly speaking, in a positional disordered structure the volume is a statistical average, which may deviate slightly from that of an ordered structure. The present calculation reveals that the deviation is negligible in the present thermodynamic scale which is further justified by the agreement of the reported experimental volumes per atom (Fig. S7).

The successful synthesis of Xe-Ni/Fe compounds in this study, well supported and corroborated by the theoretical calculations of the present and the previous study by Zhu *et al.* [1], can be attributed to the changing chemical properties of elements under pressure. This trend is clearly demonstrated by the calculated deformation charge density of $XeFe_3$ and $XeNi_3$, defined as the difference between the charge density of the crystal and the superimposed charge densities of non-interacting atoms (Figs. 4a and 4b). In both cases, electrons are removed from Xe (positive regions, red) and transferred to the metals (negative regions, blue). According to previous theoretical studies (*e.g.* [1, 7]), application of pressure dramatically affects the chemical properties of elements. Fe and Ni in particular, become highly

electronegative and can act as oxidants in compounds. Xe, on the other hand, opens up the fully filled $5p$ states as valence states. The charge transfer therefore takes place between the Xe $5p$ states and the partially filled Fe/Ni $3d$ or $4s$ (if a s to d transition occurs in Fe/Ni) states. Mulliken's analysis of electron density reveals the amounts of transferred charge in XeFe$_3$ and XeNi$_3$ are 0.64 e/Xe and 0.52 e/Xe, respectively, at 200 GPa. A greater amount of charge transfer in XeFe$_3$, which is visible in Fig. 4(a), is consistent with a lower occupation (d^6) in the $3d$ states of Fe as compared to the d^8 occupation of Ni. The different amounts of charge transfer also likely affect the reaction pressures for these two compounds.

Our experiments document that stable compounds of metals and NGEs can exist under pressure, stabilized by a major electron transfer from Xe to Fe and Ni. For comparison, much lower electron transfers between Na-He (-0.174e/He) and Cs-Xe (-0.14-0.18e/Xe) were calculated in the cases of the synthesized Na$_2$He [8] and predicted CsXe$_2$ [4] compounds, respectively. This highlights a bonding scheme that is quite different of the ones in the cases of: a) Van der Waals Xe-H$_2$ and Xe-N$_2$ compounds stabilized at elevated pressures [31, 32] and b) compounds between alkali and alkali earth metals and NGEs. This bonding pattern resembles more the bonding between high-Z NGEs, such as Xe and Kr, and strong electronegative elements such as F [33, 34], Cl and O [35] at ambient pressure. Thus, our study signifies a near halogen-like behavior of Fe and Ni under high-pressure conditions in agreement with theoretical predictions [1, 7].

The possible formation of stable Xe-Fe compounds at Earth's core thermodynamic conditions was previously considered [1, 10, 18] as a possible explanation of Xe depletion in the Earth's atmosphere. Although our study provides the first experimental evidence of the stability of Xe-Fe compounds at relevant thermodynamic conditions, it is unlikely that such compounds have been formed during the Earth's core accretion. The formation pressure of such compounds (200GPa), as determined in this work, is too high compared to that suggested for the Earth's core accretion pressure (near 50 GPa) using geochemical arguments [36]. Moreover, Mars atmosphere is also depleted in Xe while martian core pressure is $\sim$40 GPa while it is plausible to assume that Xe depletion likely stems from the same process for both planets. This suggests that the formation of XeFe$_3$ is an unlikely explanation of the "missing Xe paradox" and thus, alternative, to the Earth's core reservoir, scenarios should be considered [17]. Alternatively, a two step mechanism should be considered: an increased solubility of Xe in molten Fe at lower accretion pressures followed by a reaction at higher
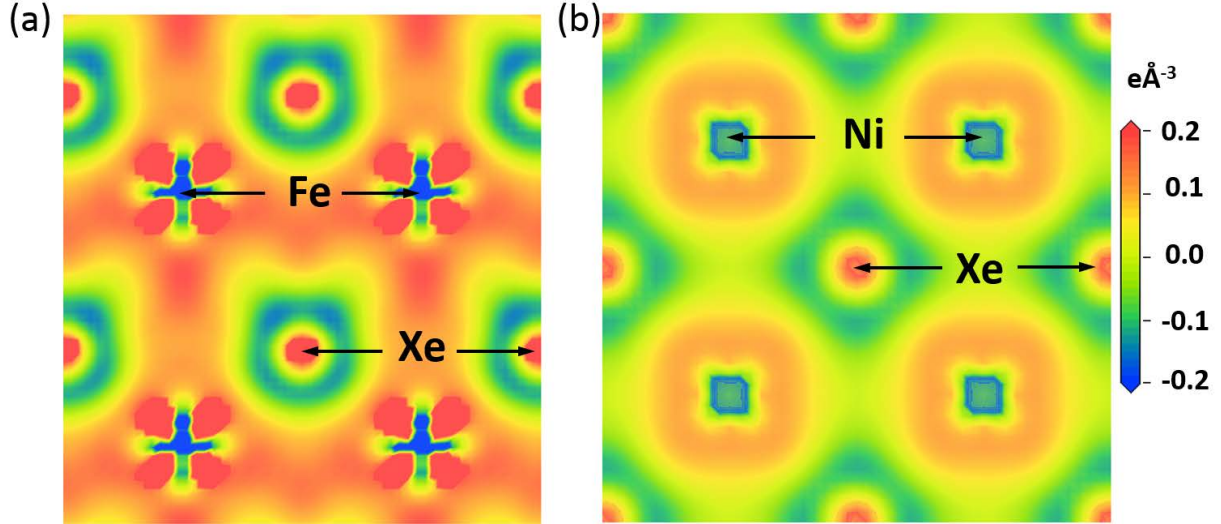
FIG. 4. Calculated deformation charge density of XeFe$_3$ in the (010) plane (a) and XeNi$_3$ in the (001) plane (b) at 200 GPa.

pressures. However, this extends beyond the scope of this work and calls for follow-up relevant studies.

HPSynC, APS.

The authors declare no competing financial interests.

————

* stavrou1@llnl.gov

† yansun.yao@usask.ca

‡ agoncharov@carnegiescience.edu

[1] L. Zhu, H. Liu, C. J. Pickard, G. Zou, and Y. Ma, Nat. Chem. **6**, 644 (2014).

[2] X. Li, A. Hermann, F. Peng, J. Lv, Y. Wang, H. Wang, and Y. Ma, Sci. Rep. **5**, 16675 (2015).

[3] M.-S. Miao, X.-l. Wang, J. Brgoch, F. Spera, M. G. Jackson, G. Kresse, and H.-q. Lin, J. Am. Chem. Soc. **137**, 14122 (2015).

[4] S. Zhang, H. Bi, S. Wei, J. Wang, Q. Li, and Y. Ma, J. Phys. Chem. C **119**, 24996 (2015).

[5] W. Grochala, R. Hoffmann, J. Feng, and N. W. Ashcroft, Angew. Chem. Int. Ed. **46**, 3620 (2007).

[6] Q. Zhu, D. Y. Jung, A. R. Oganov, C. W. Glass, C. Gatti, and A. O. Lyakhov, Nat. Chem. **5**, 61 (2013).

[7] G. Q. X. Dong, A. R. Oganov, Q. Z. X-F. Zhou, and H.-T. Wang, ArXiv e-prints , arXiv:1503.00230 (2015).

[8] X. Dong, A. R. Oganov, A. F. Goncharov, E. Stavrou, S. Lobanov, G. Saleh, G.-R. Qian, Q. Zhu, C. Gatti, V. L. Deringer, R. Dronskowski, X.-F. Zhou, V. B. Prakapenka, Z. Konôpková, I. A. Popov, A. I. Boldyrev, and H.-T. Wang, Nat. Chem. **9**, 440445 (2017).

[9] N. Dauphas, Icarus **165**, 326 (2003).

[10] K. K. M. Lee and G. Steinle-Neumann, J. Geophys. Res. **111**, B02202 (2006).

[11] E. Anders and T. Owen, Science **198**, 453 (1977).

[12] S. S. Shcheka and H. Keppler, Nature **490**, 531 (2012).

[13] C. Sanloup, S. A. Bonev, M. Hochlaf, and H. E. Maynard-Casely, Phys. Rev. Lett. **110**, 265501 (2013).

[14] C. Sanloup, B. C. Schmidt, E. M. C. Perez, A. Jambon, E. Gregoryanz, and M. Mezouar, Science **310**, 1174 (2005).

[15] M. I. J. Probert, J. Ph. Condens. Matter. **22**, 025501 (2010).

[16] A. Dewaele, N. Worth, C. J. Pickard, R. J. Needs, S. Pascarelli, O. Mathon, M. Mezouar, and

T. Irifune, Nat. Chem. **8**, 784 (2016).

[17] W. A. Caldwell, J. H. Nguyen, B. G. Pfrommer, F. Mauri, S. G. Louie, and R. Jeanloz, Science **277**, 930 (1997).

[18] D. Nishio-Hamane, T. Yagi, N. Sata, T. Fujita, and T. Okada, Geophys. Res. Lett. **37**, L04302 (2010).

[19] A. Dewaele, C. M. Pépin, G. Geneste, and G. Garbarino, High Pres. Res. **37**, 137 (2017).

[20] E. Stavrou, M. J. Zaug, J. Crowhurst, S. Lobanov, F. G. Alexander F Goncharov, V. Prakapenka, C. Presche, Y. Y. , H. Liu, and Z. Dai, in *American Geophysical Union, Fall Meeting* (2015).

[21] L. Dubrovinsky, N. Dubrovinskaia, O. Narygina, I. Kantor, A. Kuznetzov, V. B. Prakapenka, L. Vitos, B. Johansson, A. S. Mikhaylushkin, S. I. Simak, and I. A. Abrikosov, Science **316**, 1880 (2007).

[22] W. F. Bottke, D. Nesvorny, R. E. Grimm, A. Morbidelli, and D. P. O'Brien, Nature **439**, 821 (2006).

[23] See Supplemental Material at , which includes Refs. [37-54], methods, procedure followed for the identification of the *Pmmn* (1) phase and supplemental figures 1-8.

[24] H. K. Mao, Y. Wu, L. C. Chen, J. F. Shu, and A. P. Jephcoat, J. Geophys. Res. **95**, 21737 (1990).

[25] E. Stavrou, S. Lobanov, H. Dong, A. R. Oganov, V. B. Prakapenka, Z. Kon??pkov??, and A. F. Goncharov, Chem. Mater. **28**, 6925 (2016).

[26] V. V. Struzhkin, D. Y. Kim, E. Stavrou, T. Muramatsu, H.-k. Mao, C. J. Pickard, R. J. Needs, V. B. Prakapenka, and A. F. Goncharov, Nat. Comm. **7**, 12267 (2016).

[27] L. V. Pourovskii, J. Mravlje, M. Ferrero, O. Parcollet, and I. A. Abrikosov, Phys. Rev. B **90**, 155120 (2014).

[28] A. P. Jephcoat, H. k. Mao, L. W. Finger, D. E. Cox, R. J. Hemley, and C. s. Zha, Phys. Rev. Lett. **59**, 2670 (1987).

[29] V. Ozolins, C. Wolverton, and A. Zunger, Phys. Rev. B **57**, 6427 (1998).

[30] Z. W. Lu, S.-H. Wei, A. Zunger, S. Frota-Pessoa, and L. G. Ferreira, Phys. Rev. B **44**, 512 (1991).

[31] M. Somayazulu, P. Dera, A. F. Goncharov, S. A. Gramsch, P. Liermann, W. Yang, Z. Liu, H.-k. Mao, and R. J. Hemley, Nat. Chem. **2**, 50 (2010).

[32] R. T. Howie, R. Turnbull, J. Binns, M. Frost, P. Dalladay-Simpson, and E. Gregoryanz, Sci. Rep. **6**, 34896 (2016).

[33] H. H. Claassen, H. Selig, and J. G. Malm, J. Am. Chem. Soc. **84**, 3593 (1962).

[34] P. A. Agron, A. A. Mason, H. A. Levy, G. M. Begun, C. G. Jones, and D. F. Smith, Science **139**, 842 (1963).

[35] D. F. Smith, J. Am. Chem. Soc. **85**, 816 (1963).

[36] J. Li and C. B. Agee, Nature **381**, 686 (1996).

[37] C. Prescher and V. B. Prakapenka, High Pres. Res. **35**, 223 (2015).

[38] W. Kraus and G. Nolze, J. Appl. Crystallogr. **29**, 301 (1996).

[39] A. C. Larson and R. B. V. Dreele, *GSAS: General Structure Analysis System Report LAUR 86-748*, Tech. Rep. (Los Alamos National Laboratory, 2000).

[40] A. Boultif and D. Louër, J. Appl. Crystallogr. **37**, 724 (2004).

[41] V. B. Prakapenka, A. Kubo, A. Kuznetsov, A. Laskin, O. Shkurikhin, P. Dera, M. L. Rivers, and S. R. Sutton, High Pres. Res. **28**, 225 (2008).

[42] M. Kunz, A. MacDowell, W. Caldwell, D. Cambie, R. Celestre, E. Domning, R. Duarte, A. Gleason, J. Glossinger, N. Kelez, D. Plate, T. Yu, J. Zaug, H. Padmore, R. Jeanloz, A. Alivisatos, and S. Clark, J. Synchrotron Radiat. **12**, 650 (2005).

[43] E. Stavrou, M. Ahart, M. F. Mahmood, and A. F. Goncharov, Scientific Reports **3**, 1290 (2013).

[44] G. Kresse and J. Hafner, Phys. Rev. B **47**, 558 (1993).

[45] G. Kresse and D. Joubert, Phys. Rev. B **59**, 1758 (1999).

[46] J. P. Perdew, K. Burke, and M. Ernzerhof, Phys. Rev. Lett. **77**, 3865 (1996).

[47] R. Martoňák, A. Laio, and M. Parrinello, Phys. Rev. Lett. **90**, 075503 (2003).

[48] R. Martoňák, D. Donadio, A. R. Oganov, and M. Parrinello, Nat Mater **5**, 623 (2006).

[49] A. Fonari and S. Stauffer, *vaspraman.py* (https://github.com/raman-sc/VASP/, 2013).

[50] B. C. Giessen and N. J. Grant, Acta Crystallogr. **17**, 615 (1964).

[51] P. Lazor, *Phase diagrams, elasticity and thermodynamics of Ni, Co and Fe under high Pressure*, Ph.D. thesis, Uppsala University (1994).

[52] S. Merkel, A. F. Goncharov, H.-k. Mao, P. Gillet, and R. J. Hemley, Science **288**, 1626 (2000).

[53] A. F. Goncharov, E. Gregoryanz, H. K. Mao, R. J. Hemley, N. Boctor, and E. Huang., *Raman scattering of metals to very high pressures, High-Pressure Phenomena, Proceedings of*

the *International School of Physics , Enrico Fermi Course CXLVII*, edited by R. J. Hemley, M. Bernasconi, L. Ulivi, and G. Chiarotti (IOS Press, 2002).

[54] Y. A. Freiman, A. F. Goncharov, S. M. Tretyak, A. Grechnev, J. S. Tse, D. Errandonea, H.-k. Mao, and R. J. Hemley, Phys. Rev. B **78**, 014301 (2008).